

CMS Conference Report

02 October 2006

Inclusive SUSY Searches using Missing Energy plus multijets in pp collisions at $\sqrt{s} = 14$ TeV with CMS

T. Yetkin¹⁾

Department of Physics, Çukurova University, Adana, 01330, Turkey.

M. Spiropulu

European Laboratory for Nuclear Search CERN, Geneva, Switzerland.

On Behalf of the CMS collaboration

Abstract

An inclusive analysis strategy for SUSY searches in pp collisions at $\sqrt{s} = 14$ TeV with the CMS detector is discussed. The missing transverse energy plus multijets canonical signature is used. Emphasis is put in methods to normalize the backgrounds using the data and in understanding the experimental systematic uncertainties. A 5σ excess can be observed with $O(\text{pb}^{-1})$ at a particular low mass SUSY point. The 5σ discovery reach contours in the mSUGRA parameter space for 1 and 10 fb^{-1} are obtained.

Presented at Physics at LHC Conference, 3-8 July 2006, Krakow, Poland.

¹⁾ Present Address: Department of Physics, Mersin University, Mersin, 33343, Turkey

1 Introduction

One of the most compelling and robust extensions of the Standard Model [1] is supersymmetry (SUSY) [2]. For simplicity the *minimal* construction (MSSM) is often used to link SUSY with the Standard Model [3]. The most general MSSM would induce proton decay with a weak-interaction lifetime; to avoid this, baryon and lepton conservation are enforced in the MSSM by postulating a new conserved quantity, R -parity, $R = (-1)^{3(B-L)+2s}$, where for each particle s is the spin, and B and L are the respective baryon and lepton assignments. R -parity conservation leads to characteristic SUSY signatures with missing transverse energy in the final state due to the stable lightest supersymmetric particle (LSP).

We consider gluino (the fermionic partners of gluons) and squark (the bosonic partners of quarks) production in pp collisions at $\sqrt{s} = 14$ TeV within the minimal supergravity model (mSUGRA)[3]. In this model the entire SUSY mass spectrum is essentially determined by only five unknown parameters: the common scalar mass at the GUT scale, M_0 ; the common gaugino mass at the GUT scale, $M_{1/2}$; the common trilinear coupling at the GUT scale, A_0 ; the sign of the Higgsino mixing parameter, $sign(\mu)$; and the ratio of the Higgs vacuum expectation values, $\tan\beta$. The search for the production and decay of gluinos and squarks is using the large missing transverse energy plus multijet signature. The large missing energy originates from the two LSPs in the final states of the squark and gluino decays. The three or more hadronic jets result from the hadronic decays of the \tilde{q} and/or \tilde{g} .

2 Data Samples

For the SUSY signal event generation the Monte Carlo program ISAJET (v7.69) [4] interfaced with PYTHIA (v6.225) [5] (which provides the parton shower and underlying event model) is used. The analysis is performed at the CMS test point “LM1” ([6], [7]) with parameters $M_0 = 60 \text{ GeV}c^2$, $M_{1/2} = 250 \text{ GeV}c^2$, $A_0 = 0$, $\mu > 0$ and $\tan\beta = 10$. For this set of parameters $m(\tilde{g}) > m(\tilde{q})$ the production of $\tilde{g}\tilde{q}$ is 53%, $\tilde{q}\tilde{q}$ 28% and $\tilde{g}\tilde{g}$ 12%. The decay $\tilde{g} \rightarrow q_{L,R} + q$ is dominant. Some of the resulting masses are $m(\tilde{g}) \sim 600 \text{ GeV}c^2$, $m(\tilde{q}) \sim 550 \text{ GeV}c^2$, and $\chi_1^0 \sim 120 \text{ GeV}c^2$. The total leading order production cross section for squarks and gluinos with the given mSUGRA parameters is ~ 50 pb.

The major Standard Model background processes include production of Z +jets with the Z decaying invisibly, W +jets, top-antitop pairs, dibosons, single top and QCD jets. The single top sample (containing only the most significant t -channel production) is generated with TopReX 4.11 [8]. The remaining Standard Model backgrounds are produced inclusively using PYTHIA.

Unless otherwise stated, the data samples used in this analysis were simulated with the CMS GEANT4-based simulation OSCAR [9] and reconstructed using the detailed CMS reconstruction ORCA [10].

2.1 Jet and Missing Transverse Energy Reconstruction

The CMS detector is described in detail in [11]. The momenta of charged particles are measured in the silicon and pixel tracking devices which are positioned inside a 4 T superconducting solenoidal magnet. The central and end-cap electromagnetic and hadronic calorimeters (also within the magnet) are arranged in a semi-projective tower geometry, cover the pseudorapidity region $|\eta| < 3$ [11] and are used to identify jets. Jets are defined as localized energy depositions in the calorimeters and are reconstructed using an iterative clustering algorithm with a fixed cone of radius $\Delta R \equiv \sqrt{\Delta\eta^2 + \Delta\phi^2} = 0.5$ in $\eta - \phi$ space [11]. Jets are ordered in transverse energy, $E_T = E \sin\theta$, where E is the scalar sum of energy deposited in the calorimeter towers within the cone, and θ is the angle formed by the beam-line, the event vertex, and the cone center. Jets with $E_T > 30$ GeV and with $|\eta| < 3$ are used throughout this analysis. The jet corrections described in section 3.3 are not applied at this stage.

The offline missing transverse energy is defined as the negative vector sum of the transverse energy in the electromagnetic and hadronic calorimeter towers, $\vec{E}_T^{miss} = -\sum_i (E_i \sin\theta_i) \hat{n}_i$, where E_i is the energy of the i -th tower, \hat{n}_i is a transverse unit vector pointing to the center of each tower, and θ_i is the polar angle of the tower; the sum extends to $|\eta| < 5$. The data sample is selected with a hardware trigger which requires $E_T^{miss,L1} > 46$ GeV ($|\eta| < 5$ coverage) and a central jet of $E_T > 88$ GeV. A parametrization of the L1 trigger efficiency as measured in a dijet sample is applied to all data analyzed. For the confirmation of the High Level Trigger (HLT) the E_T^{miss} is required to be above 200 GeV where the HLT trigger is fully efficient. The details of L1 and HLT triggers and application to this analysis can be found at [11, 12]. In the following sections we detail the methodology and analysis strategies toward a search for SUSY using a dataset of events collected according to the missing transverse energy plus jet L1 and HLT trigger path.

Table 1: Cleanup pre-selection efficiency.

Sample/Requirement	$F_{em} > 0.1$	$F_{ch} > 0.175$	Both(%)
LM1	99.88%	91.32%	91.24%

3 Data Clean-up and Analysis Path

3.1 Event Electromagnetic and Event Charged Fraction

In anticipation of real data, a pre-selection clean-up filter is used to reject accelerator- and detector-related backgrounds (such as beam halo and noise), and cosmic ray events. At least one primary vertex is required in the event. The event electromagnetic fraction, F_{em} (defined as the E_T -weighted jet electromagnetic fraction sum over the electromagnetic calorimeter acceptance, $|\eta_d| \leq 3.0$) and the event charged fraction, F_{ch} (defined as the sum of the P_T of the associated to the jet tracks for jets within $|\eta| < 1.7$, over the calorimetric jet transverse energy) are used in the pre-selection to distinguish real jet events from the fake jet events. The pre-selection requirements and their efficiency on the signal are shown in Table 1. The values of the requirements are chosen based on the Tevatron data clean-up [13].

3.2 Indirect Lepton Veto

In this analysis there is no explicit lepton identification. Leptons in the signal SUSY events result from cascade decays of squarks and gluinos through charginos and neutralinos. To reduce the large Standard Model background contribution mainly from $W(\rightarrow \ell\nu) + jets$, $Z(\rightarrow \ell\ell) + jets$ and $t\bar{t}$ production and decays an *indirect lepton veto* (ILV) scheme is designed. The aim of the ILV is twofold: a) to retain large signal efficiency b) to achieve large rejection of the W , Z , $t\bar{t}$ backgrounds.

The ILV scheme uses two parts of the detector: tracker and calorimeter. In the calorimeter events are selected if the first and second highest E_T jets are not purely electromagnetic, *i.e.* $f_{em,j(1)} < 0.9$ and $f_{em,j(2)} < 0.9$. In the tracker a tracking isolation strategy is employed as follows: If the leading track in the event has $P_T \geq 15 \text{ GeV}/c$ and the ratio of the sum of the P_T of all tracks around it in a cone of $\Delta R=0.35$ over the P_T of the track is less than 10% the event is dropped. In the analysis path table below this requirement is noted as Iso^{lead trk=0}

The cumulative W/Z +jets rejection efficiency when both requirements of the ILV are applied is between 50% and 90% depending on the lepton flavour, with lower rejection as expected when the boson decay product includes a τ lepton. When applied in the full analysis path the ILV rejects 40% of $t\bar{t}$ inclusive events. The cumulative SUSY signal efficiency is $\sim 80\%$.

3.3 Missing Transverse Energy in QCD Production

Due the very high QCD production cross section the SM background to a large missing transverse energy plus jets data-sample is dominated by QCD events. The observed missing transverse energy in QCD jet production is largely a result of jet mis-measurements and detector resolution.

In this study, topological requirements are designed to eliminate as much as possible the QCD contribution. Well measured QCD dijet events with back-to-back in ϕ jet topology are used for obtaining jet corrections. These are well balanced events with low missing transverse energy. Large missing energy in QCD events originates from jet mis-measurements. In such events the highest E_T jet is typically the most accurately measured. When any jet in the event is mis-measured, usually the second or third jet, the E_T^{miss} direction is pulled close in ϕ to the mis-measured jet direction. We eliminate such residual QCD component by using the correlation in the $\delta\phi_1 = |\phi_{j(1)} - \phi(E_T^{miss})|$ versus $\delta\phi_2 = |\phi_{j(2)} - \phi(E_T^{miss})|$ plane. Events with $R_1 > 0.5$ rad and $R_2 > 0.5$ rad, where $R_1 = \sqrt{\delta\phi_2^2 + (\pi - \delta\phi_1)^2}$ and $R_2 = \sqrt{\delta\phi_1^2 + (\pi - \delta\phi_2)^2}$, are accepted. In addition we require that no jet in the event be closer than 0.3 rad to the missing energy direction and that the second jet be further than 20° from it.

After a baseline selection of $N_j \geq 2$ and $E_T^{miss} > 93 \text{ GeV}$ the cumulative efficiency of the angular requirements is $\sim 90\%$ for the SUSY signal. They reject $\sim 85\%$ of all QCD events.

3.4 The Standard Z Boson Candle Calibration

Events with large missing transverse energy and ≥ 3 jets in the final state are expected from $Z(\rightarrow \nu\bar{\nu}) + \geq 3$ jets and $W(\rightarrow \tau\nu) + \geq 2$ jets (the third jet originating from the hadronic τ decay) processes. Additional residual contribution is expected also from $W(\rightarrow \mu\nu, e\nu) + \geq 3$ jets. A comprehensive normalization program is developed that relies on the Z +multijet data to accurately estimate the W and Z +multijet background contribution in a large E_T^{miss} plus multijet search.

The Monte Carlo predictions for events with ≥ 3 jets and Z boson $P_T > 200$ GeV/c will be normalized to the observed $Z(\rightarrow \mu\mu) + 2$ jets data sample (where Z boson $P_T > 200$ GeV/c) via the measured $R = \frac{dN_{events}}{dN_{jets}}$ ratio, where dN_{events} is the number of events accumulated with $\sim 1 \text{ fb}^{-1}$ of data.

The ratio $\rho \equiv \frac{\sigma(pp \rightarrow W(\rightarrow \mu\nu) + jets)}{\sigma(pp \rightarrow Z(\rightarrow \mu^+ \mu^-) + jets)}$ will be used to normalize the W +jets Monte Carlo predictions. By normalizing the MC predictions to data large systematic effects are avoided that are due to the renormalization scale, the choice of parton density functions, initial- and final-state radiation, and the jet energy scale. The total uncertainty ($\sim 5\%$) is then dominated by the uncertainty on the luminosity measurement, the uncertainty on the measured ratio $R = \frac{dN_{events}}{dN_{jets}}$ (to be measured with the data), and the uncertainty on the ratio ρ as a function of the jet multiplicity, N_{jet} . The details of the normalization can be found in reference [7].

4 Analysis Path and Results

The signal to background ratio is further enhanced after clean-up pre-selection requirements in the final steps of the analysis by following the path shown in Table 2. The global signal efficiency for the analysis is $\sim 13\%$ while the signal to background ratio is ~ 26 . The results after the analysis path applied are shown in Table 3.

Table 2: The E_T^{miss} + multijet SUSY search analysis path.

Requirement	Remark
Level 1	Level-1 trigger param.
HLT, $E_T^{miss} > 200$ GeV	trigger/signal signature
primary vertex ≥ 1	primary cleanup
$F_{em} \geq 0.175, F_{ch} \geq 0.1$	primary cleanup
$N_j \geq 3, \eta_d^{1j} < 1.7$	signal signature
$\delta\phi_{min}(E_T^{miss} - jet) \geq 0.3$ rad, $R1, R2 > 0.5$ rad, $\delta\phi(E_T^{miss} - j(2)) > 20^\circ$	QCD rejection
$Isol^{lead trk} = 0$	ILV (I) $W/Z/t\bar{t}$ rejection
$f_{em(j(1))}, f_{em(j(2))} < 0.9$	ILV (II), $W/Z/t\bar{t}$ rejection
$E_{T,j(1)} > 180$ GeV, $E_{T,j(2)} > 110$ GeV	S/B optimization
$H_T \equiv E_{T(2)} + E_{T(3)} + E_{T(4)} + E_T^{miss} > 500$ GeV	S/B optimization

Table 3: Selected SUSY and SM background events for 1 fb^{-1} at LM1 .

Signal	$t\bar{t}$	single t	$Z(\rightarrow \nu\bar{\nu}) + \text{jets}$	$(W/Z, WW/ZZ/ZW) + \text{jets}$	QCD
6319	53.9	2.6	48	33	107

4.1 Systematic Uncertainties

For the major background components the systematic uncertainties are found as follows:

- $t\bar{t}$ uncertainties: 7% E_T^{miss} shape, 22% JES, 13% statistical,
- $Z \rightarrow \nu\bar{\nu} + \text{jets}, W/Z + \text{jets}$: 5% Luminosity (direct candle normalization to the data),
- QCD: E_T^{miss} 7% shape, 22% JES, 10% statistical.

Details on the systematic uncertainty estimates can be found in [7]. The number of background events per background component and their uncertainties are tabulated in Table 4.

Table 4: SM background components and uncertainties for 1 fb^{-1} .

Sample	Number of Events
$t\bar{t}$, single top	$56 \pm 11(\text{sys}) \pm 7.5(\text{stat})$
$Z(\rightarrow \nu\bar{\nu}) + \text{jets}$	$48 \pm 3.5(\text{all})$
$(W/Z, WW/ZZ/ZW) + \text{jets}$	$33 \pm 2.5(\text{all})$
QCD	$107 \pm 25(\text{sys}) \pm 10(\text{stat})$

5 SUSY Discovery Potential with $E_T^{\text{miss}} + \text{Jets}$

To perform the 5σ discovery scan in the mSUGRA parameter space CMS fast simulation FAMOS [14] is used. A high mass (“HM1”) CMS test point with the five mSUGRA parameters $M_0 = 180 \text{ GeV}/c^2$, $M_{1/2} = 850 \text{ GeV}/c^2$, $A_0 = 0$, $\mu > 0$ and $\tan\beta = 10$ ($m(\tilde{g}) \sim 1890 \text{ GeV}/c^2$, $m(\tilde{q}) \sim 1700 \text{ GeV}/c^2$) is used as optimization reference and the E_T^{miss} and H_T requirements are raised to 600 GeV and 1500 GeV correspondingly. The result is shown in Figure 1.

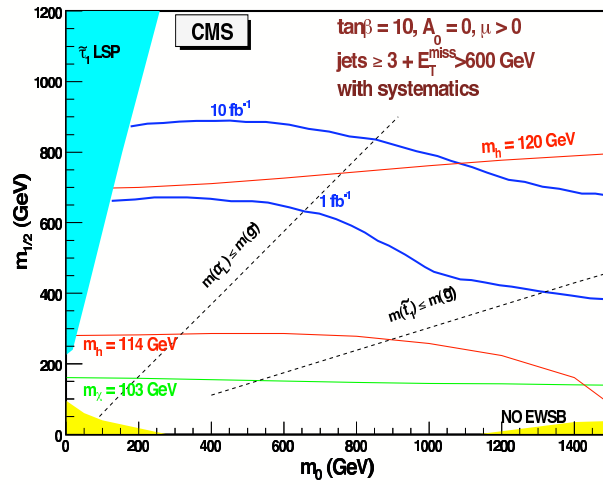


Figure 1: 5σ reach for 1 fb^{-1} and 10 fb^{-1} using multijets and missing transverse energy final state.

6 Discussion and Conclusions

Based on the SM background estimates and their uncertainties, a 5σ observation of low mass SUSY ($m(\tilde{g}) \sim 600 \text{ GeV}/c^2$) is in principle achievable with $\sim 6 \text{ pb}^{-1}$ in events with large missing energy plus multijets. With adequate data-based strategies of controlling and estimating the SM backgrounds and their uncertainties, low mass SUSY can be discovered with $0.1\text{-}1 \text{ fb}^{-1}$.

The comparison of the signal, total background and its components for the E_T^{miss} and $M_{eff} \equiv E_{T(1)} + E_{T(2)} + E_{T(3)} + E_{T(4)} + E_T^{\text{miss}}$ are shown in Figure 2 for the low mass SUSY test point LM1. The E_T^{miss} and H_T distributions comparison between the HM1 SUSY signal and SM backgrounds are shown in Figure 3 for the high mass test point HM1.

We would like to thank to the organizers of the Physics at LHC Conference for the possibility to present our work and for their hospitality. We are grateful to Gülsen Önengüt, Shuichi Kunori and Jim Freeman for supporting this analysis.

References

- [1] S. L. Glashow, Nucl. Phys. **22** 588 (1961); S. Weinberg, Phys. Rev. Lett. **19**, 1264 (1967); A. Salam, Proc. 8th Nobel Symposium, Stockholm (1979).

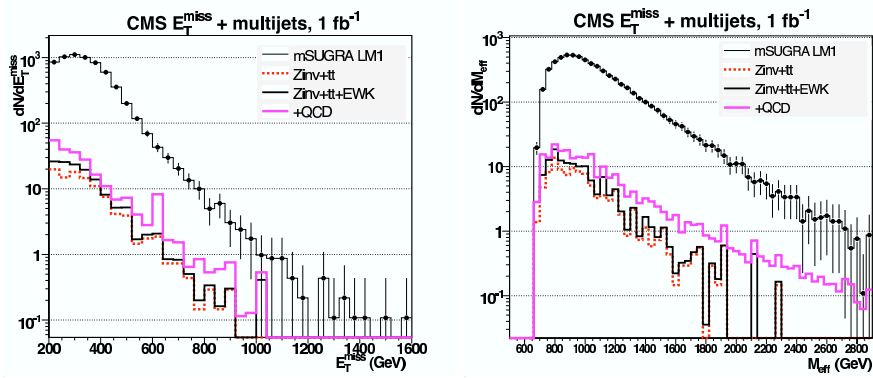


Figure 2: LM1 signal and SM background distributions for E_T^{miss} (left) and M_{eff} (right).

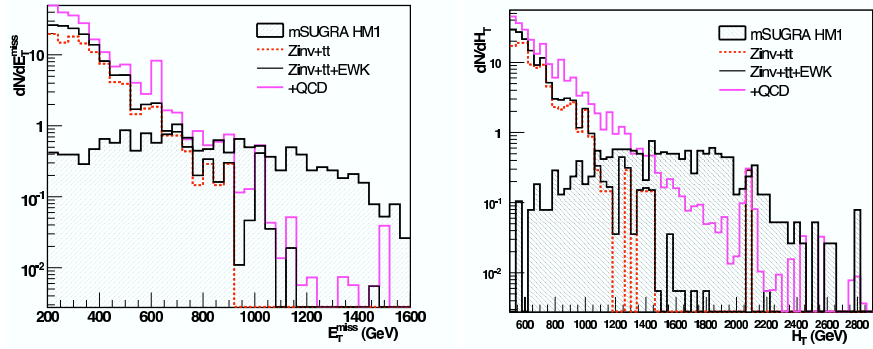


Figure 3: HM1 signal and SM background distributions (1 fb^{-1}) for E_T^{miss} (left) and H_T (right).

- [2] S. Coleman and J. Mandula, *Phys. Rev.* **159**, 1251 (1967); P. Ramond, *Phys. Rev.* **D3**, 2415 (1971); A. H. Chamseddine, R. Arnowitt, and P. Nath, *Phys. Rev. Lett.* **49**, 970 (1982); *Phys. Rev. Lett.* **50**, 232 (1983); R. Barbieri, S. Ferrara, and C. A. Savoy, *Phys. Lett.* **B119**, 343 (1982); L. Hall, J. Lykken and S. Weinberg, *Phys. Rev.* **D27**, 2359 (1983); H.P. Nilles, *Phys. Rept.* **110**, 1 (1984).
- [3] For a review see S.P. Martin, “A Supersymmetry Primer”, hep-ph/9709356 (1997), in *Perspectives on supersymmetry*, 1-98, Kane, G.L. (ed.) (1997).
- [4] H. Baer et al., ISAJET 7.69: A Monte Carlo Event Generator for pp , $\bar{p}p$, and $e^+ + e^-$ Interactions”, hep-ph/0312045 (2003).
- [5] T. Sjostrand, S. Mrenna and P. Skands, *J. High Energy Phys.*, 0605 (2006) 026.
- [6] M.Battaglia et al. *Eur. Phys. J. C* **33** (2004) 273, hep-ph/0306219.
- [7] CMS Collaboration, “The CMS Physics Technical Design Report, Volume 2: Physics Performance”, CERN/LHCC 2006-021 (2006).
- [8] S. R. Slabospitsky, L. Sonnenschein, *Comput. Phys. Commun.* , **148** (2002) 87, hep-ph/0201292, <http://sirius.ihep.su/~spitsky/toprex/toprex.html>
- [9] “Object oriented Simulation for CMS Analysis and Reconstruction”,<http://cmsdoc.cern.ch/oscar/>.
- [10] “Object oriented Reconstruction for CMS Analysis”, <http://cmsdoc.cern.ch/orca/>.
- [11] CMS Collaboration, “The CMS Physics Technical Design Report, Volume 1: Detector Performance and Software”, CERN/LHCC 2006-001 (2006).
- [12] T. Yetkin, Ph.D. Thesis (Çukurova U.), CMS TS-2006/005, March 2006, 169pp.
- [13] M. Spiropulu, Ph.D. Thesis (Harvard U.), FERMILAB-THESIS-2000-16, UMI-99-88600, Nov 2000. 338pp.

[14] <http://cmsdoc.cern.ch/famos/>.

[15] M. L. Mangano et al., J. High Energy Phys., 0307 (2003) 001.